



Comparison of Thalamus Volume on Magnetic Resonance and Cadaveric Section Images

Selim KAYACI¹, Orhan BAS², Fatma BEYAZAL CELIKER³, Yilmaz UCUNCU⁴, Yusuf Kemal ARSLAN⁵, Mehmet Faik OZVEREN⁶, Sukru AYKOL⁷

¹Erzincan Binali Yildirim University, Faculty of Medicine, Department of Neurosurgery, Erzincan, Turkey

²Ordu University, Faculty of Medicine, Department of Anatomy, Ordu, Turkey

³Recep Tayyip Erdogan University, Department of Radiology, Rize, Turkey

⁴Recep Tayyip Erdogan University, Faculty of Medicine, Department of Anatomy, Rize, Turkey

⁵Erzincan Binali Yildirim University, Faculty of Medicine, Department of Biostatistics, Erzincan, Turkey

⁶Kirikkale University, Faculty of Medicine, Department of Neurosurgery, Kirikkale, Turkey

⁷Gazi University, Faculty of Medicine, Department of Neurosurgery, Ankara, Turkey

Corresponding author: Selim KAYACI ✉ selim_kayaci@hotmail.com

ABSTRACT

AIM: To measure and to compare the volume of thalamus using magnetic resonance imaging (MRI) and the anatomical sections.

MATERIAL and METHODS: In this study, 13 brain specimens were used. First, the images were taken in 3 mm sections on MRI, the thickness of the thalamus was measured. Subsequently, 4 mm coronal sections were prepared using a microtome. The thalamic volumes calculated from cadaveric specimens were compared with the measurements obtained using MRI.

RESULTS: On MRI, the mean thalamic volumes on the right and left hemispheres were found to be $5843.4 \pm 361.6 \text{ mm}^3$ and $5377.0 \pm 666.2 \text{ mm}^3$ respectively. The mean volumes of the cadaveric sections were $5610.8 \pm 401.3 \text{ mm}^3$ on the right side and $5618.5 \pm 604.1 \text{ mm}^3$ on the left hemisphere. No statistically significant difference was found between the volume calculated from MRI and that obtained from the cadaveric section ($p < 0.05$).

CONCLUSION: This study shows a correlation between measurement of thalamus volume based on MRI and those calculated from anatomical sections. Our findings support the reliability of DBS procedures using MRI and stereotactic method.

KEYWORDS: Cadaver, Deep brain stimulation, Magnetic Resonance Imaging, Planimetry technique, Thalamus

ABBREVIATIONS: MRI: Magnetic resonance imaging, DBS: Deep brain stimulation, VIM: Ventral intermediate, PD: Parkinson's disease, IGE-GTCS: Idiopathic generalized epilepsy-generalized tonic clonic seizures

INTRODUCTION

The thalamus is an egg-like grey matter mass measuring 3 x 1.5 x 1.5 cm located in the white matter in the depths of the cerebral cortex and along the sagittal direction. The human thalamus is a nuclear complex in the diencephalon (18), and this structure is one of the four parts of the diencephalon (the epithalamus, thalamus and metathalamus, subthalamus,

and hypothalamus) (2). Thalamus supports both sensory and motor mechanisms. Thalamic nuclei (50-60 nuclei) extend toward one or several well-defined cortical areas (18). More than one cortical area receives afferents from a single thalamic nucleus and transmits information to different thalamic nuclei. The corticofugal projection provides positive feedback to the "correct" input, simultaneously suppressing irrelevant

Selim KAYACI

: 0000-0003-1303-7569

Orhan BAS

: 0000-0002-7449-2699

Fatma BEYAZAL CELIKER : 0000-0002-5420-9825

Yilmaz UCUNCU

: 0000-0001-9453-5425

Yusuf Kemal ARSLAN

: 0000-0003-1308-8569

Mehmet Faik OZVEREN : 0000-0001-7768-1519

Sukru AYKOL : 0000-0001-7896-1563

information (18). Topographical organization of the thalamic afferents and efferents is contralateral, and the lateralization of the thalamic functions affects both sensory and motoric aspects (18).

Abnormalities of the basal ganglia and thalamus may be detected on neuroimaging in a wide variety of pathological conditions. The causes of these abnormalities may be broadly classified as systemic or focal, some of which may have an acute onset while others may show slow progression. The deep grey matter nuclei may be affected by toxic poisoning (by carbon monoxide, methanol and cyanide) and systemic metabolic abnormalities (e.g. liver disease, hyper- or hypoglycemia, hypoxia, Leigh disease, Wilson disease, osmotic myelinolysis and Wernicke's encephalopathy). Certain degenerative conditions (e.g. Huntington disease, neurodegeneration with brain iron accumulation, Creutzfeldt Jakob disease and Fahr disease) and vascular abnormalities (venous infarction and arterial occlusion) also have a predilection for involving the basal ganglia and thalamus. Finally, some focal inflammatory conditions and infections (Neuro-Behçet disease, flavivirus encephalitis and toxoplasmosis) or neoplasms (primary central nervous system lymphoma and primary bilateral thalamic glioma) may also affect the basal ganglia and thalamus on both sides (17).

Symptoms of lesions located in the thalamus are closely related to the function of the areas involved (18). Damage to the ventero-postero-lateral and ventero-postero-medial nuclei; usually results in contralateral hemianesthesia. Typically, all somatic sensory modalities including: light touch, conscious proprioception, two-point discrimination and vibration, pain and temperature are affected. The loss of all somatic sensory modalities is an important diagnostic marker for thalamic damage (lesion that disrupt sensory function often affect different functions at different rates and generally do not affect pain sensation). Involvement of the lateral geniculate body leads to contralateral homonymous hemianopsia (18). If thalamic damage extends to the ventero-anterior/ventero-lateral nucleus complex, it may lead to contralateral movement disorders. Which can occur in the form of cerebellar damage (ataxia and intentional tremor) or basal ganglion damage (choreoathetoid movements) (18).

Functional neurosurgery is one of the fastest growing areas of neurosurgery. It started with ablative procedures initially that were gradually replaced with nonablative interventions such as deep brain stimulation (DBS). DBS is a widely used minimally invasive and reversible method to treat various neurological and psychiatric disorders by stimulating deep located structures in the brain (26). Implantation of electrodes into targets which are not visible in current imaging methods can be performed using stereotactic principles (26).

It is known that different clinical manifestations occur in lesions of different nuclei of thalamus. Therefore, the targeted thalamus nuclei in their treatment are different (13). Ventral intermediate (VIM) nucleus of the thalamus is considered the target in the treatment of Parkinson's disease (PD) and essential tremor (23). However the use of VIM DBS for PD is less frequent because of the recognition of other more

effective target nuclei (subthalamic nucleus and globus pallidus internus) (13). VIM DBS has also been reported to relieve orthostatic tremor (15). Thalamic DBS has been used in the treatment for Tourette syndrome (31). Wherein bilateral thalamic centromedian/parafascicular complex is considered the target (30). The treatment of intractable pain is one of the oldest indications for DBS. Several different targets have been used, one of them is the sensory thalamus (29). Besides these; medically intractable seizures have been treated using DBS of the anterior or centromedian nucleus of the thalamus (3).

The most profound development in the surgical treatment of extrapyramidal system disorders after neurostimulation procedures is the development of stereotactic imaging modalities. Stereotaxy is an objective localization method that applied during DBS for neurophysiological control of the target. Although the DBS applied with stereotaxy is a minimally invasive procedure, it has some complications along with prolonged duration of surgery (16,19). If the microelectrode system is not properly positioned, the target anatomic point may not be correctly localized.

To what extent is it possible to accurately detect the thalamus during DBS? To understand this, comparison of the volumetric measurements of the thalamus with cranium MRI and the volume measured on cadaveric specimens may be useful. For this reason, in this study, the thalamus volume were first radiologically calculated and then compared using anatomical sections the results were evaluated in terms of DBS procedures.

■ MATERIAL and METHODS

This study was performed after the approval of Recep Tayyip Erdogan University Clinical Ethics Committee on 10/07/2016 (no: 70). The study was conducted on 15 adult human cadaveric brain specimens which were removed on autopsy. The age, sex, or disease status of these cadavers were unknown. These cadaveric specimens were approximately 10 years old and were fixed in 10% formaldehyde. Two of the cadaveric specimens were excluded from the study. One of them was pediatric cadaver and the other had intense artifact during MRI. For the remaining 13 specimens, images were first taken using a MRI device with 3 mm sections (Figure 1A, B). The specimens were then buried in agar and 4 mm thick sections were prepared from these specimens using a slicing machine.

MRI Data

Imaging of the cadavers was performed using a 36 channel 1.5 T MRI device (Discovery MR 750w, GEM-70, General Electric Company, USA). TSE (T1 FLAIR). Images were obtained for each cadaver (3 mm cross-section) using head coils. Image parameters were as follow: TR: 2310, TE: 8.1/Ef, EC: 1/135.7 kHz, TI: 974, Head 24/FL:a, FOV: 24x21.6, 2.00 thk/1.00 sp, 60/06:25, and 320 x 224/2.00 NEX. The number of sections on which the thalamus appeared on MR images was calculated. Onis 2.5 [Onis Free Edition 2.5 Download (Free) - Onis.exe] and Image J ([https://imagej.net/ Downloads](https://imagej.net/Downloads)) software were then used to calculate thalamus volume from the MR images. Onis 2.5 is an analytical program that rapidly converts images

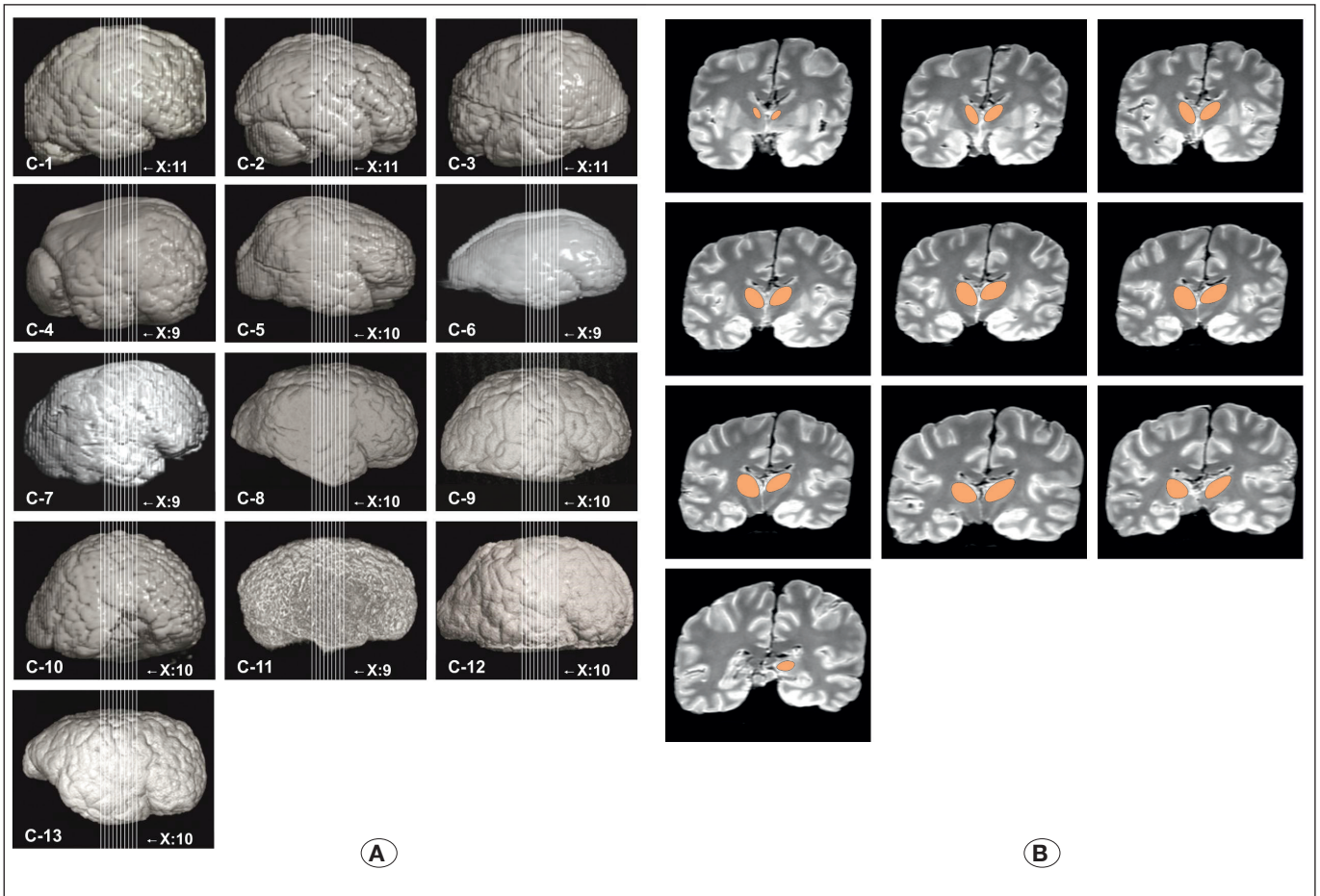


Figure 1: A) Lateral plane volume rendering of the cadavers MR images (C: cadaver, X: number of cross sections which display thalamus). **B)** Display of thalamus on MRI for the 5th cadaver (frontal plane).

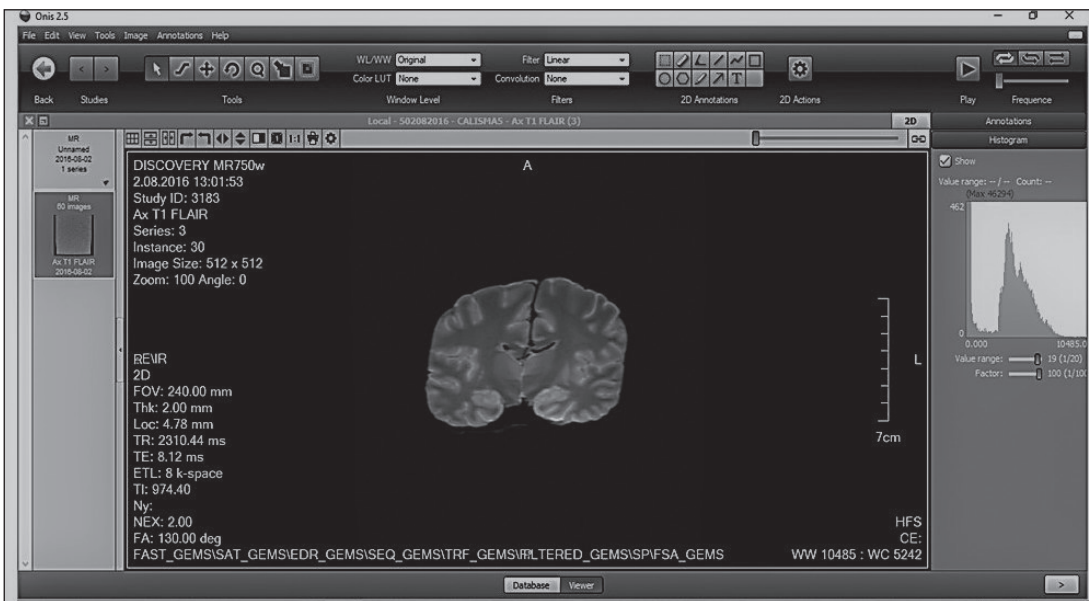


Figure 2: Onis 2.5 analysis program.

into DICOM format in a serial manner (Figure 2). Image J software constitutes image analysis used in image processing and surface area calculation in clinical and scientific studies (Figure 3).

Preparation of Cadaver Specimens

Agar (Trypticase Soy Agar, Merck) was prepared for processing of the specimens. For this process, 1.5% of powdered agar was added to pure water and mixed. This mixture was melted in boiling water bath. The autoclave was prepared by sterilizing at 121°C and then cooling to 50°C. The agar specimens were laid in plastic boxes and allowed to solidify for 6 hours at room temperature. Slicing Machine (Bosch MAS9454M) was used for cutting specimens and 4 mm thick coronal sections were prepared (Figure 4A, B). Sections thinner than 4 mm could not be obtained because the samples were broken. The obtained sections were scanned (Scan, PC, HP, ProDesk 600, G2, MT, USA) using a scanner (Xerox, Workcentre 7428, USA). The total number of sections taken from each cadaver and the number of sections in which thalami were seen were noted. The Image J program was used to adjust the scale and calculate the surface area on these images (Figure 5).

Calculation of the Volume according to the Cavalieri Principle

Thalamus MR images and cadaveric cross-sectional views were used to calculate volumes using Cavalieri principle and planimetry technique. Surface area of the thalamus on MR images converted to cadaver and DICOM format in volume calculations were calculated by planimetry method using Image J program. The surface areas for the volume calculation were estimated in all sections taken from the thalamus without any sampling. Each measurement was performed blindly by the same person at least three times and the mean value was considered. The measurement was performed using sections of a randomly picked specimen each time. MRI and cadaveric cross-sectional images of the same specimen were not allowed to be sequential. In other words, the person who performed the measurement was not allowed to correlate between surface volumes of MRI and cadaveric images. The thalamus volume was calculated by summarizing the sum of surface areas in the following formula, as described previously (1).

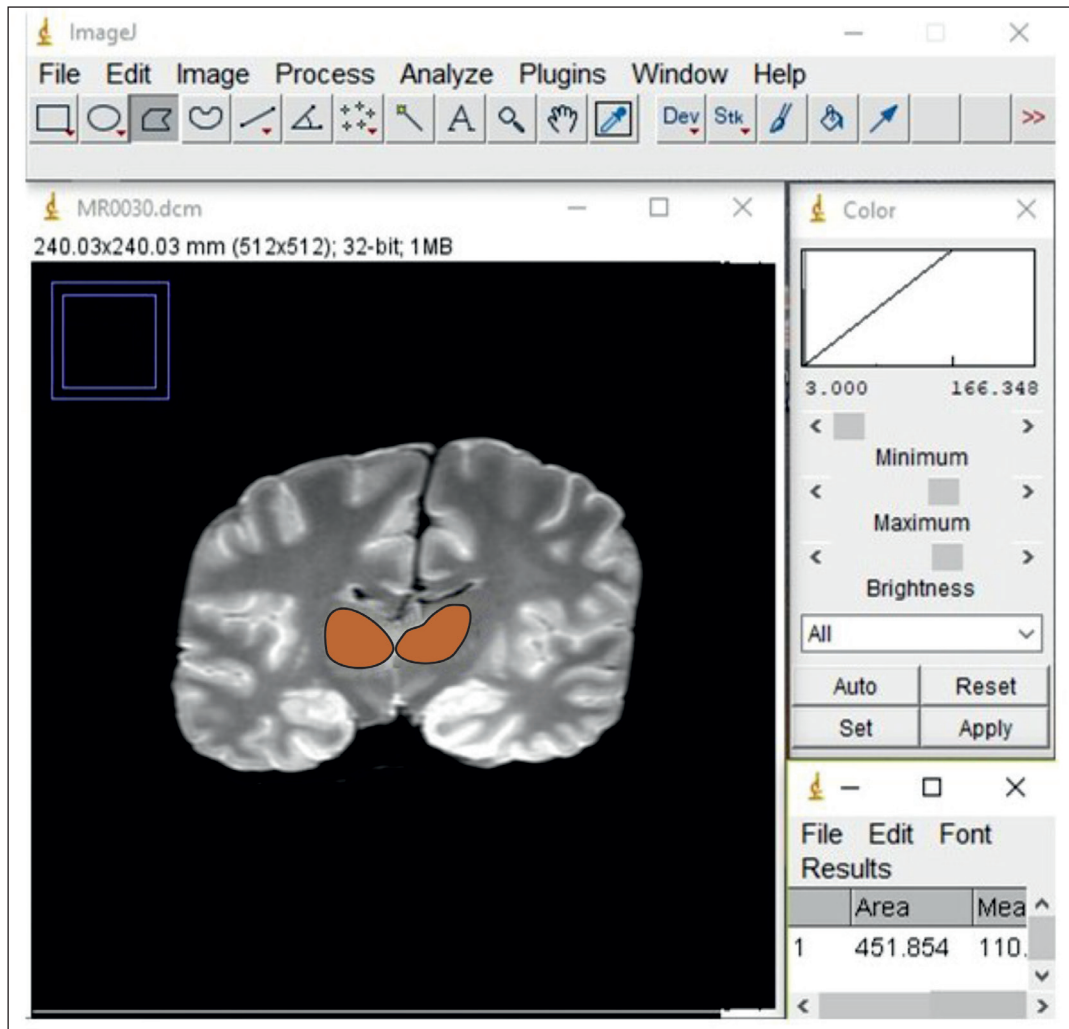


Figure 3: Image J analysis program.

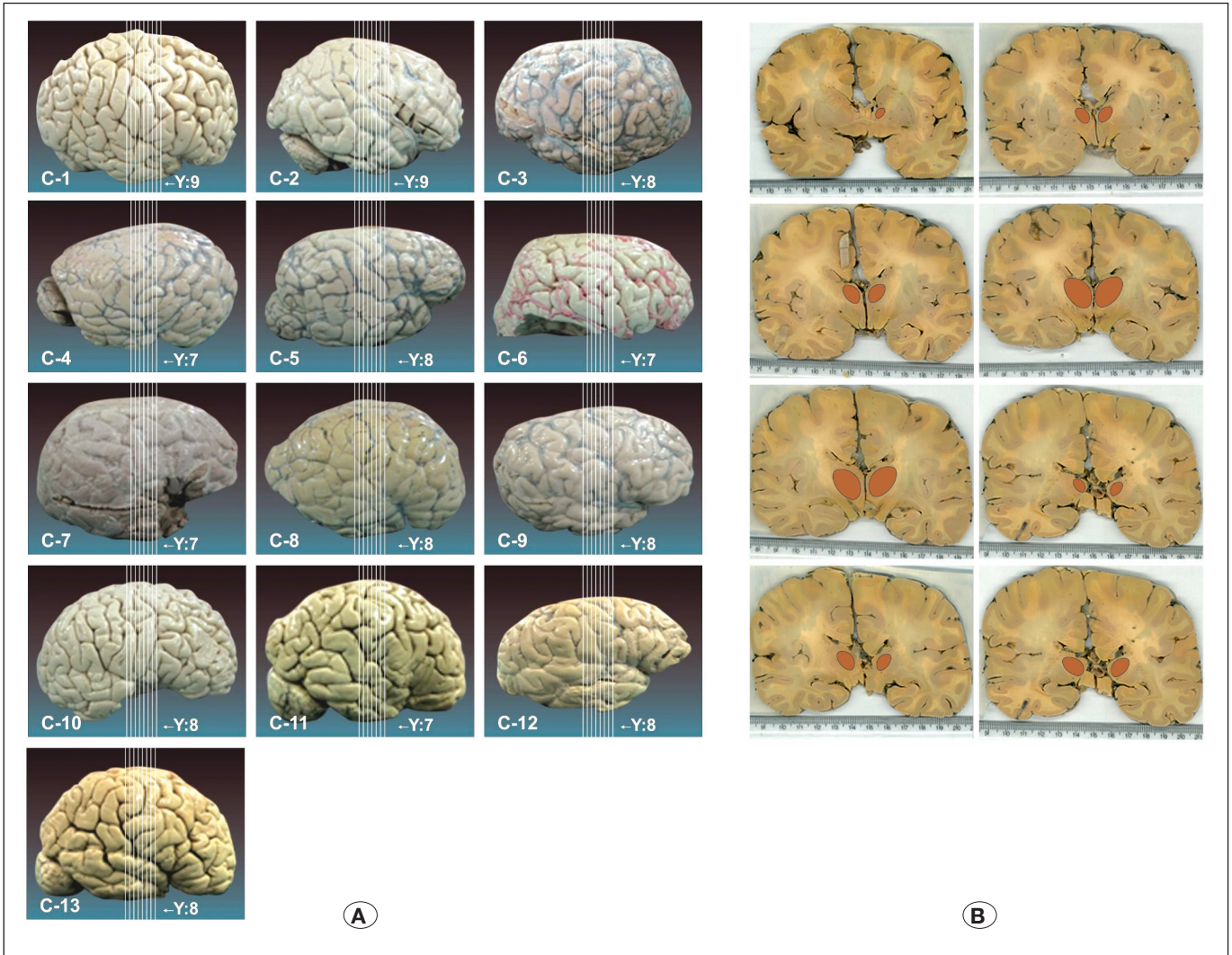


Figure 4: **A)** Lateral plane views of the cadavers (**C:** cadaver; **Y:** number of cross-sections which display thalamus). **B)** Display of thalamus for the 5th Cadaver on frontal plane.

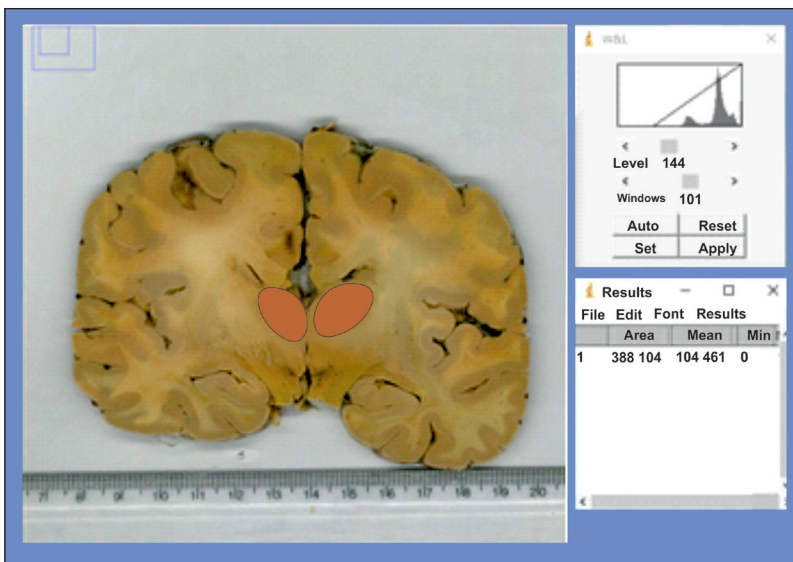


Figure 5: Calculation of surface area of cadaver sections with Image J program.

$$V = t \times \Sigma A$$

In the above equation, t denotes the thickness of the consecutive sections and ΣA denotes the total surface area of the thimble in the section view. All data were entered into a Microsoft Excel spread sheet which automatically calculated the values based on the above formula. The volume of each brain hemisphere was calculated separately.

Statistical Analysis

Data pertaining to continuous variables are presented as mean \pm standard deviation and/or median (min–max). Comparisons between the right-sided and left-sided measurements were performed using paired sample t test. Firstly, the relation between MRI measurements and cadaveric measurements was analysed with the Pearson correlation coefficient and results were presented as $r(p)$; subsequently, the reliability analysis was performed. While performing reliability analysis, the two-way mixed effects model was used where people effects were random and measured effects were fixed for intraclass correlation coefficient with absolute agreement. A p value <0.05 was considered to be statistically significant. Statistical analysis was performed using the IBM SPSS v19 program (IBM Software, New York, United States).

RESULTS

A total of 694 (min: 48, max: 58) sections were obtained on MRI and a total of 477 (min: 34, max: 42) sections on cadaveric section. The number of cross-sections on MRI which displayed thalamus was 127 (min: 8, max: 11) on the right side and 126 (min: 9, max: 11) on the left side. The number of sections of the cadaveric section showing the thalamus was 102 (min: 7, max: 9) on the right side and 99 (min: 7, max: 9) on the left side (Table I). Table II shows the MRI and volumetric measurements obtained from the cadaveric sections. The mean thalamus volume on MRI was 5843.4 ± 361.6 mm³ (range: 5328.0–6576.0 mm³) on the right side and 5377.0 ± 666.2 mm³ (range: 4295.0–6539.0 mm³) on the left side. In the cadaveric specimens, the mean thalamus volume was 5610.8 ± 401.3 mm³ (range: 5020.0–6476.0 mm³) on the right side and 5618.5 ± 604.1 mm³ (range: 4820.0–6748.0 mm³) on the left side. The agreement between the two measurement techniques for right thalamus was statistically significant ($p < 0.001$). Intraclass correlation coefficient was $\rho = 0.797$, which indicates an excellent agreement. Similarly, for the left thalamus, agreement between the two measurement techniques was statistically significant ($p = 0.006$). Intraclass correlation coefficient was $\rho = 0.619$, which suggests good agreement between the two measurement techniques. Cadaveric right and left thalamus volumes were similar ($p = 0.946$); however, MRI showed a statistically significant difference between the right and left thalamus volumes ($p = 0.014$) (Table III).

DISCUSSION

For accurate diagnoses and treatment of brain diseases, it is necessary to understand the brain structures in 3D and to make volumetric measurements. Two-dimensional (2D) tools (e.g. anatomy books) or traditional 3D tools (e.g. plastic models)

are not enough to understand the 3D structures of the brain. For this purpose, high-resolution MRI methods are important. MRI-based volume measurement is now increasingly used to investigate neuroanatomical structures in patients with neurological and psychiatric disorders such as schizophrenia, Alzheimer's disease and epilepsy (1,5,6,20,27). In many studies, automatic segmentation methods using MR images have been defined. Calmon and Roberts reported a segmentation method for lateral ventricles in coronal MR (9). Stokking et al. developed morphology-based brain segmentation using T1-weighted MRI images for fully automated segmentation (32). Webb et al. reported an automatic method for the detection of hippocampal atrophy (36). Each of these methods is based on fragmentation of the target object in each MR image obtained in different sequences.

The thalamus is investigated in many neurological and neuropsychiatric disorders using MRI. However, because the texture contrast between the grey and white matter in the thalamic region is weak, it is difficult to obtain volumetric measurements of the thalamus (22). Development of improved high-resolution MR devices has helped overcome this challenge.

Literature review revealed several studies on volumetric analysis of thalamus based on MRI (7,12,22,28,37). Csernansky et al. investigated the shape and volume of the thalamus in schizophrenic patients based on MRI. In schizophrenic patients, the mean thalamus volumes on the right and left sides were 7350 mm³ (SD=846) and 7307 mm³ (SD=790), respectively; the corresponding values in normal humans were 7734 mm³ and 7702 mm³ (SD=851), respectively. They concluded that the reduction in thalamus volume was not significant when considering the decrease in the total brain volume in schizophrenia patients (12). Using the Freesurfer method and stereological technique, Keller et al. calculated the thalamus volume by 3D T1-weighted MRI and 3T MRI and assessed the consistency between these methods. Among these methods, there was no significant difference in the thalamus volumes (22). Wiegell et al. performed diffusion-tensor MRI morphometric analysis of the thalamus by automatic segmentation method; the mean volumes of the thalamus on the left and right sides were 7141 ± 530 mm³ and 7073 ± 457 mm³, respectively (37).

Wang et al. compared the morphological and functional degenerative changes in the thalamus in patients with idiopathic generalized epilepsy-generalized tonic clonic seizures (IGE-GTCS) and healthy controls; patients with IGE-GTCS showed significantly decreased grey matter volume in the bilateral thalamus (specifically in the medial dorsal nucleus and pulvinar), orbit frontal cortex, insular and cerebellum (35). Conversely, Betting et al. found an increase in volume in the anterior thalamus in patients with IGE (7). Rao et al. found that the volumes of the right and left thalamus in schizophrenic patients were significantly lower than those in the healthy group (28).

In the present study, the thalamus volume was found to be 5377.0 ± 662.2 mm³ on the left and 5843.4 ± 361.6 mm³ on the right side. These values are lower than the results of Csernansky and Wiegell, and are higher than the results of Rao et al. (12,28,37).

Table I: Section Numbers of MRI and Cadaveric Specimens (n=13)

| Cadaver | The total section number on MRI | The total section number on Cadaver | The number of sections of right thalamus on MRI | The number of sections of left thalamus on MRI | The number of sections of right thalamus on cadaver | The number of sections of left thalamus on cadaver |
|--------------|---------------------------------|-------------------------------------|---|--|---|--|
| 1 | 58 | 42 | 11 | 11 | 9 | 9 |
| 2 | 56 | 38 | 11 | 10 | 9 | 8 |
| 3 | 55 | 38 | 10 | 11 | 8 | 8 |
| 4 | 51 | 36 | 9 | 9 | 7 | 7 |
| 5 | 52 | 37 | 10 | 9 | 8 | 7 |
| 6 | 54 | 36 | 9 | 9 | 7 | 7 |
| 7 | 52 | 36 | 9 | 9 | 7 | 7 |
| 8 | 50 | 35 | 10 | 10 | 8 | 8 |
| 9 | 55 | 36 | 10 | 10 | 8 | 8 |
| 10 | 54 | 37 | 10 | 10 | 8 | 8 |
| 11 | 48 | 34 | 8 | 9 | 7 | 7 |
| 12 | 54 | 34 | 10 | 9 | 8 | 7 |
| 13 | 55 | 38 | 10 | 10 | 8 | 8 |
| Total number | 694 | 477 | 127 | 126 | 102 | 99 |
| Min-Max | 48.0-58.0 | 34.0-42.0 | 8.0-11.0 | 9.0-11.0 | 7.0-9.0 | 7.0-9.0 |

Table II: MRI and Cadaver Thalamus Volumes (mm³) (n=13)

| Cadaver | MRI | | Cadaveric section | |
|-----------|----------------|----------------|-------------------|----------------|
| | Right | Left | Right | Left |
| 1 | 5902.0 | 4562.0 | 5728.0 | 5332.0 |
| 2 | 5686.0 | 4791.0 | 5508.0 | 5768.0 |
| 3 | 5566.0 | 4881.0 | 5424.0 | 5568.0 |
| 4 | 6101.0 | 5637.0 | 5712.0 | 6364.0 |
| 5 | 5835.0 | 4295.0 | 5652.0 | 5020.0 |
| 6 | 6306.0 | 6539.0 | 5928.0 | 6304.0 |
| 7 | 5456.0 | 4295.0 | 5208.0 | 4820.0 |
| 8 | 5328.0 | 5361.0 | 5020.0 | 5060.0 |
| 9 | 6576.0 | 5912.0 | 6476.0 | 6748.0 |
| 10 | 5580.0 | 5512.0 | 5052.0 | 5120.0 |
| 11 | 6188.0 | 5756.0 | 6020.0 | 5548.0 |
| 12 | 5640.0 | 5444.0 | 5504.0 | 5248.0 |
| 13 | 5800.0 | 6286.0 | 5708.0 | 6140.0 |
| Mean ± SD | 5843.4 ± 361.6 | 5377.0 ± 666.2 | 5610.8 ± 401.3 | 5618.5 ± 604.1 |
| Median | 5800.0 | 5444.0 | 5652.0 | 5548.0 |
| Min-max | 5328.0-6576.0 | 4295.0-6539.0 | 5020.0-6476.0 | 4820.0-6748.0 |

Table III: Volume of Thalamus with Different Measurement Techniques (MRI and Cadaveric section)

| | Measurement Technique | | r(p)** |
|----------------|--|--|---------------|
| | Cadaveric section | MRI | |
| Thalamus right | 5610.8 ± 401.3 5652.0 (5020.0-6476.0) | 5843.4 ± 361.6 5800.0 (5328.0-6576.0) | 0.95 (<0.001) |
| Thalamus left | 5618.5 ± 604.1 5548.0 (4820.0-6748.0) | 5377.0 ± 666.2 5444.0 (4295.0-6539.0) | 0.65 (0.016) |
| p* | 0.946 | 0.014 | |

*Paired samples test for Right-Left, **Correlation between MRI-Cadaver.

The cadaveric brain specimens used in the present study were removed from the skull, flushed with 10% formaldehyde and stored for about 10 years. Preservation of cadaveric specimens in formaldehyde may cause them to shrink and reduce in volume (21,25,33). The storage of specimens in formaldehyde for a long time may have caused the shrinkage of brain and thalamus. This may explain our lower values than the MRI-based volumetric measurements reported in literature.

In addition, there was a significant difference between the measurements of right and left thalamus based on MRI in this study. The right and left hemispheres of the human brain are known to be anatomically and functionally asymmetric. The asymmetry between the volumes of right and left basal nuclei is well documented (34,38). However, this alone cannot entirely explain the difference observed in our study. Another possible reason for the observed difference may be the position of cadaveric specimens during MRI and the possibility of superimposition during imaging (4,10).

In literature, volumetric analysis of the thalamus based on cadaveric sections has rarely been reported. Chung and Kim performed a study on cadaveric brain in Korea as a post-mortem. They first immersed the specimen in gelatin solution and then segmented it in various planes on MRI and visualized the basal nuclei and other structures. Then they used the virtual section program on the same cadaver. They found that this virtual dissection program facilitated a better understanding of the location and shape of brain components in 3D (11). Byne et al. examined the post-mortem volume and neurone numbers in the thalamus of patients with schizophrenia. They reported a median thalamus volume of 4610 ± 0.514 mm³. They found no significant change in the total thalamus volume, with changes in volume and neurone numbers (8).

Various stereological methods have been developed to perform volumetric analysis of structures in the cadaver brain. The Cavalieri method is one of the most reliable and frequently used methods. The Cavalieri principle provides a highly sensitive and unbiased method for quantitative measurements (14,24). In this principle, parallel and equally thick portions of an object are taken, and the volume is calculated by the total number of cross-sectional areas and cross-sectional thickness. CT, MR or ultrasonography cross-sectional imaging

can be used to calculate the volume of an object using the Cavalieri principle (1). Because of these properties, we used the Cavalieri method for volumetric measurements of cadaveric specimens. We examined 13 adult cadaveric brain specimens in this study. The specimens were segmented in 1.5T MR devices, and after measuring thalamus volume, we prepared cadaveric sections and compared the thalamus volume stereologically. However, we can say that the actual values were calculated in the volumetric analysis using the Cavalieri method.

Importance of this Study

The present study aimed to compare the thalamus volume measurements obtained on both MRI and cadaveric sections. Our results demonstrated a correlation between the two measurements. What is the relevance of this in terms of DBS? Despite being a nonablative and minimally invasive procedure, DBS may cause some complications and side effects. Regarding the implementation of the electrode system, complications such as cranial infection, brain abscess, system malfunction, system displacement and system misplacement can be encountered. This procedure may also lead to complications such as intracranial hemorrhage, venous infarction, postoperative dyskinesia, postoperative behavior, cognitive dysfunction, air embolism and suicidal tendency (16). Incorrect placement of the system results from the lack of ability to determine the target with precision. In this context, the volume values obtained on MRI and from the cadaveric anatomical sections are important in stereotactic procedures. As we have shown in our study, these values are close to each other and there is a strong correlation between these two measurements. We, therefore, believe that the complications encountered during DBS may be due to the practitioner’s inexperience or carelessness.

CONCLUSION

The main finding of this study is the significant correlation between thalamus measurements based on MRI and volumetric measurements based on anatomical sections. Our findings support the reliability of the DBS procedure using MRI accompanied by stereotactic method despite some complications.

■ ACKNOWLEDGEMENTS

We thank Dr. Kazim Sahin for helping to prepare the cadaveric specimens. We would also like to thank Prof. Dr. Vahdet Gul for his support in English translation.

■ REFERENCES

1. Acer N, Sahin B, Bas O, Ertekin T, Usanmaz M: Comparison of three methods for the estimation of total intracranial volume: Stereologic, planimetric, and anthropometric approaches. *Ann Plast Surg* 58:48–53, 2007
2. Afifi Adel K, Bergman Ronald A. *Functional neuroanatomy: Text and Atlas*, 2nd ed. 2005:156
3. Andrade DM, Zumsteg D, Hamani C, Hodaie M, Sarkissian S, Lozano AM, Wennberg RA: Long-term follow-up of patients with thalamic deep brain stimulation for epilepsy. *Neurology* 66:1571–1573, 2006
4. Auer T, Schwarcz A, Horváth RA, Barsi P, Janszky J: Functional magnetic resonance imaging in neurology. *Ideggyogy Sz* 30: 16-23, 2008
5. Bas O, Acer N, Mas N, Karabekir HS, Kusbeci OY, Sahin B: Stereological evaluation of the volume and volume fraction of intracranial structures in magnetic resonance images of patients with Alzheimer's disease. *Ann Anat* 191:186-195, 2008
6. Bernasconi F, Andermann DL, Arnold Bernasconi A: Entorhinal cortex MRI assessment in temporal, extratemporal, and idiopathic generalized epilepsy. *Epilepsia* 44:1070-1074, 2003
7. Betting LE, Mory SB, Lopes-Cendes I, Li LM, Guerreiro MM, Guerreiro CA, Cendes F: MRI volumetry shows increased anterior thalamic volumes in patients with absence seizures. *Epilepsy Behav* 8:575-580, 2006
8. Byne W, Buchsbaum MS, Mattiace LA, Hazlett EA, Kemether E, Elhakem SL, Purohit DP, Haroutunian V, Jones L: Postmortem assessment of thalamic nuclear volumes in subjects with schizophrenia. *Am J Psychiatry* 159:59-65, 2002
9. Calmon G, Roberts N: Automatic measurement of changes in brain volume on consecutive 3D MR images by segmentation propagation. *Magn Reson Imaging* 18:439-453, 2000
10. Chapman PH, Buchbinder BR, Cosgrove GR, Jiang HJ: Functional magnetic resonance imaging for cortical mapping in pediatric neurosurgery. *Pediatr Neurosurg* 23:122-126, 1995
11. Chung MS, Kim SY: Three-dimensional image and virtual dissection program of the brain made of Korean cadaver. *Yonsei Med J* 41:299-303, 2000
12. Csernansky JG, Schindler MK, Splinter NR, Wang L, Gado M, Selemon LD, Rastogi-Cruz D, Posener JA, Thompson PA, Miller MI: Abnormalities of thalamic volume and shape in schizophrenia. *Am J Psychiatry* 161:896-902, 2004
13. Dormont D, Seidenwurm D, Galanaud D, Cornu P, Yelnik J, Bardinet E: Neuroimaging and deep brain stimulation. *AJNR Am J Neuroradiol* 31:15-23, 2010
14. Gundersen HJ, Jensen EB: The efficiency of systematic sampling in stereology and its prediction. *J Microsc* 147: 229-263, 1987
15. Guridi J, Rodriguez-Oroz MC, Arbizu J, Alegre M, Prieto E, Landeche I, Manrique M, Artieda J, Obeso JA: Successful thalamic deep brain stimulation for orthostatic tremor. *Mov Disord* 23:1808–1811, 2008
16. Hariz MI: Complications of deep brain stimulation surgery. *Mov Disord* 17:162-166, 2002
17. Hegde AN, Mohan S, Lath N, Lim CC: Differential diagnosis for bilateral abnormalities of the basal ganglia and thalamus. *Radiographics* 31:5-30, 2011
18. Herrero MT, Barcia C, Navarro JM: Functional anatomy of thalamus and basal ganglia. *Childs Nerv Syst* 18:386-404, 2002
19. Ho NC, Andreasen P, Nopoulos S, Arndt V, Magnotta Flaum M: Progressive structural brain abnormalities and their relationship to clinical outcome: A longitudinal magnetic resonance imaging study early in schizophrenia. *Arch Gen Psychiatry* 60:585–594, 2003
20. Honey CR, Berk C, Palur RS, Schulzer M: Microelectrode recording for pallidotomy: Mandatory, beneficial or dangerous? *Stereotact Func Neurosurg* 77: 98-100, 2001
21. Jonmarker S, Valdman A, Lindberg A, Hellström M, Egevad L: Tissue shrinkage after fixation with formalin injection of prostatectomy specimens. *Virchows Arch* 449: 297-301, 2006
22. Keller SS, Gerdes JS, Mohammadi S, Kellinghaus C, Kugel H, Deppe K, Ringelstein EB, Evers S, Schwindt W, Deppe M: Volume estimation of the thalamus using freesurfer and stereology: Consistency between methods. *Neuroinformatics* 10: 341-350, 2012
23. Lee JY, Kondziolka D: Thalamic deep brain stimulation for management of essential tremor. *J Neurosurg* 103:400–403, 2005
24. Mayhew TM, Gundersen HJG: If you assume, you can make an ass out of u and me: A decade of the disector for stereological counting of particles in 3D space. *J Anat* 188:1-15, 1996
25. Mouritzen Dam A: Shrinkage of the brain during histological procedures with fixation in formaldehyde solutions of different concentrations. *J Hirnforsch* 20:115-119, 1979
26. Möttönen T, Katisko J, Haapasalo J, Tähtinen T, Kiekara T, Kähärä V, Peltola J, Öhman J, Lehtimäki K: Defining the anterior nucleus of the thalamus (ANT) as a deep brain stimulation target in refractory epilepsy: Delineation using 3T MRI and intraoperative microelectrode recording. *Neuroimage Clin* 5: 823-829, 2015
27. Murphy TL, Jernigan TL, Fennema-Notestine C: Left hippocampal volume loss in Alzheimer's disease is reflected in performance on odor identification: A structural MRI study. *J Int Neuropsychol Soc* 9:459-471, 2003
28. Rao NP, Kalmady S, Arasappa R, Venkatasubramanian G: Clinical correlates of thalamus volume deficits in anti-psychotic-naïve schizophrenia patients: A 3-Tesla MRI study. *Indian J Psychiatry* 52: 229-235, 2010
29. Raslan AM: Deep brain stimulation for chronic pain: Can it help? *Pain* 120:1–2, 2006
30. Savica R, Stead M, Mack KJ, Lee KH, Klassen BT: Deep brain stimulation in tourette syndrome: A description of 3 patients with excellent outcome. *Mayo Clin Proc* 87:59-62, 2012

31. Servello D, Porta M, Sassi M, Brambilla A, Robertson MM: Deep brain stimulation in 18 patients with severe Gilles de la Tourette syndrome refractory to treatment: The surgery and stimulation. *J Neurol Neurosurg Psychiatry* 79:136-142, 2008
32. Stokking R, Vincken KL, Viergever MA: Automatic morphology-based brain segmentation (MBRASE) from MRI-T1 data. *Neuroimage* 12:726-738, 2000
33. Quester R, Schröder R: The shrinkage of the human brain stem during formalin fixation and embedding in paraffin. *J Neurosci Methods* 75:81-89, 1997
34. Vernaleken I, Weibrich C, Siessmeier T, Buchholz HG, Rösch F, Heinz A, Cumming P, Stoeter P, Bartenstein P, Gründer G: Asymmetry in dopamine D(2/3) receptors of caudate nucleus is lost with age. *Neuroimage* 34:870-878, 2006
35. Wang Z, Zhang Z, Jiao Q, Liao W, Chen G, Sun K, Shen L, Wang M, Li K, Liu Y, Lu G: Impairments of thalamic nuclei in idiopathic generalized epilepsy revealed by a study combining morphological and functional connectivity MRI. *PLoS One* 7(7):e39701, 2012
36. Webb J, Guimond A, Eldridge P, Chadwick D, Meunier J, Thirion JP, Roberts N: Automatic detection of hippocampal atrophy on magnetic resonance images. *Magn Reson Imaging* 17(8):1149-1161, 1999
37. Wiegell MR, Tuch DS, Larsson HB, Wedeen VJ: Automatic segmentation of thalamic nuclei from diffusion tensor magnetic resonance imaging. *Neuroimage* 19: 391-401, 2003
38. Yamashita K, Yoshiura T, Hiwatashi A, Noguchi T, Togao O: Volumetric asymmetry and differential aging effect of the human caudate nucleus in normal individuals: A prospective MR imaging study. *J Neuroimaging* 21:34-37, 2011